Nonlinear atomic Fabry-Perot interferometer: From the mean-field theory to the *atom blockade* effect

I. Carusotto
Scuola Normale Superiore and INFM, Piazza dei Cavalieri 7, 56126 Pisa, Italy
(Received 27 March 2000; revised manuscript received 20 June 2000; published 16 January 2001)

We have investigated nonlinear atom optical effects which arise from atom-atom collisional interactions in a single-mode atomic Fabry-Perot cavity driven by a coherent cw atom laser beam. When the nonlinear interaction energy per single atom is small, the exact numerical solution of the master equation is well reproduced by a mean-field treatment in which quantum fluctuations are included linearizing the stochastic equations of the Positive-P representation. On the other hand, when the damping of the cavity mode is very weak and its wave-function is tightly confined in space, a regime of strong nonlinearity can be achieved. For the specific case of an incident atom laser frequency at resonance with the empty cavity, the numerical calculations predict a sort of *atom blockade* effect, which is a sort of atom optical analog of the well-known Coulomb blockade effect of electronic transport through microscopic structures: only one atom can occupy the cavity mode at a time and the statistical properties of the transmitted beam, being very similar to the resonance fluorescence from a single two-level system, show definitely nonclassical behaviors such as antibunching. Only at very large incident intensities, more than one atom can be simultaneously forced inside the cavity mode: in this regime, the results of the numerical calculations can be successfully interpreted using a dressed cavity model. From the formal analogy between atomic matter waves and optical light waves in nonlinear media, it follows that the same results hold for photonic systems.

DOI: 10.1103/PhysRevA.63.023610 PACS number(s): 03.75.Dg, 03.75.Fi, 42.50.Dv, 42.65.−k

I. INTRODUCTION

Since the realization in 1995 of atomic Bose-Einstein condensates (BEC) [1], atom optics has begun to exploit the accumulation of a macroscopic number of atoms in the same quantum state in order to generate coherent matter waves which are the atomic analog of laser light [2]. Very recently, such *atom laser* beams have started to be used for experiments in nonlinear atom optics [3], in which the classical wave character of the atom laser pulses plays a fundamental role. The atomic analog of the nonlinear susceptibility of optical media is given by atom-atom interactions [4,5]: two-body elastic collisions are in fact responsible for a nonlinear cubic term in the atomic field evolution equation of the same form as a Kerr nonlinear refractive index [6].

Meanwhile, a large amount of theoretical work has been devoted to the study of a number of different nonlinear atom optical effects in various configurations, such as atomic four-wave mixing [7], atom optical limiting and atom optical bistability [8]. For the observation of this latter effect, in particular, new models of atomic Fabry-Perot (FP) resonators have been proposed [8], which are predicted to give an enhanced mode spacing and more tightly confined mode wave-functions with respect to previous proposals [9].

In recent years, since the development of photonic cavities with very large Q-factors [10,11] and optical materials with very strong nonlinearities [12], a large interest has been devoted by the (photon) optical community to the search for optical schemes in which nonlinear optical effects are triggered by a very small number of photons [13,14]. In such systems, in fact, the quantum state of the field can be manipulated down to the single quantum level and definitely nonclassical states can be generated [15].

Thanks to the formal analogy between light waves in Kerr-like nonlinear media and Bose matter waves, similar effects are expected to occur in atom optical systems: both the light and the matter fields are in fact described by operators obeying Bose statistics and in both cases the interactions introduce cubic terms in the wave equation. In addition, since the collisional atom-atom interactions are generally much stronger than the photon-photon interactions mediated by the underlying nonlinear medium, atom optics is expected to be an even more favorable field for the study of definitely quantum optical effects. For example, the switching threshold for optical bistability in the atomic FP described in [8] has been predicted to be as low as a few 10^{13} at/cm^2 s, which in the case of visible light corresponds to intensities of the order of μW/cm^2.

In the present article we investigate the coherence properties of the transmitted beam through a single-mode atomic Fabry-Perot interferometer when this is illuminated by a monochromatic and coherent atom laser beam: the field dynamics is numerically studied by solving the full quantum master equation for the cavity mode and the results obtained are physically interpreted by comparing them with the available approximate theories.

As expected, mean-field theory (MFT) [16] is found to give accurate results in the weak nonlinearity case, i.e., when an appreciable nonlinear modulation of the transmission requires the presence of a large number of atoms in the cavity mode. Within MFT, the atomic Bose field is considered as a classical $\boldsymbol{C}$-number field and its fluctuations around the classical steady-state are treated in a linearized way by means of the stochastic differential equations of Positive-P representation [17] in their linearized form [18].

In the opposite strong nonlinearity case, when the transmission state is substantially modified by the presence of a single atom in the cavity mode, the discrete nature of the matter field is important: MFT, which is based on a classical field assumption, breaks down and a full quantum calculation

is necessary in order to accurately describe the peculiar nonclassical properties of the transmitted beam.

For the specific case of an incident field at resonance with the empty cavity mode, the numerical solution of the full master equation predicts a sort of *atom blockade* effect, which reminds one of the well-known Coulomb blockade effect of electronic transport through microscopic structures: if the electrostatic potential change following the injection of a single carrier is able to substantially affect the injection of the successive carriers, the current shot-noise is strongly suppressed [19]. Analogously, atom-atom interactions in our FP cavity can be so strong that the presence of a single atom shifts the mode frequency off-resonance from the incident atom laser beam and the following atoms are effectively forbidden from resonantly entering the cavity before the first atom has left. For moderate incident intensities, the cavity therefore behaves as a two-level system and the transmitted atomic beam has the usual nonclassical properties of resonance fluorescence light, such as a strong antibunching [20,21]. Only at very large incident intensities—much larger than the saturation intensity of the effective two-level system—more than one atom can be forced to be in the cavity mode at the same time and a peculiar dependence on the incident intensity is found for both the coherent and the incoherent transmission. In this regime, some of the most peculiar features resulting from the numerical calculation are well explained by a dressed cavity model [22,23], in particular the frequencies of the incoherent transmission peaks.

Most of the present discussion concerns cases in which the nonlinearity gives rise to an optical limiter behavior; effects related to atom optical bistability are postponed to a forthcoming publication.

In Sec. II, we shall introduce the Hamiltonian of the model and we shall describe the physical processes involved, as well as the physical parameters which control them. In Sec. III we shall address the weak nonlinearity case, in which the full numerical calculation is well reproduced by MFT with a linearized treatment of fluctuations. In Sec. IV, we shall discuss the results obtained for the opposite case of a strong nonlinearity. Finally, Sec. V is devoted to conclusions and future work.

II. THE MODEL

Consider a quasi-cw beam of atoms coherently extracted [2] from a trapped Bose-Einstein condensate (BEC) by means of a radio-frequency field or of a pair of optical beams in a Raman configuration. Thanks to the coherent nature of the outcoupling mechanism used to transfer atoms from the trapped BEC to the propagating beam, the all-order coherence of the BEC transfers into a similar property for the *atom laser* beam. If the intensity of the outcoupled beam is weak and the number of atoms in the trapped BEC large, the depletion rate of the BEC is very slow and the outcoupled beam can be considered as having a weak but constant intensity as well as a constant frequency; this limitation on the atom laser intensity could clearly be overcome if the BEC were continuously replenished, making a true atom laser. Provided phase diffusion of the condensate occurs on a time scale much longer than any of the characteristic time scales

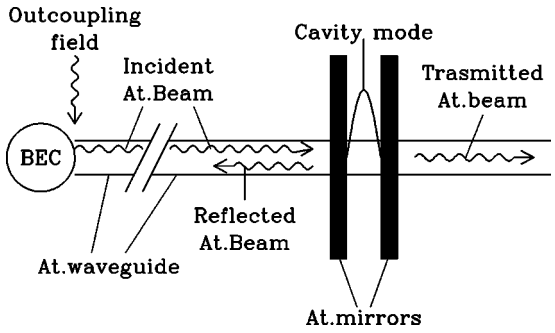

FIG. 1. Sketch of the experimental scheme under examination.

of the nonlinear cavity, the atom laser beam can be modeled as a monochromatic classical ***C***-number wave [24].

As shown in Fig. 1, suppose we inject such an outcoupled wave into a single mode atomic waveguide [25] in order to freeze the transverse atomic motion; in this way, the system behaves as a one-dimensional one. At the same time, the use of a horizontal waveguide allows us to counteract the effect of gravity, so that the longitudinal wavefunction of the outcoupled beam is simply a plane wave $\psi(x,t) = \psi_i e^{i(k_L x - \omega_L t)}$ of frequency ω_L and momentum k_L.

Suppose now we send such a cw coherent atomic beam onto an atomic Fabry-Perot (FP) cavity, formed by a pair of parallel atomic mirrors which confine atomic matter waves in the space between them; atomic motion between the mirrors is quantized in discrete cavity modes, which are coupled to externally propagating modes because of the nonperfect reflectivity of the cavity mirrors. Several simple schemes which realize such a device have been proposed, most of which are based on the optical potential applied to the atoms by far off-resonance laser fields: some of them [9] use a blue detuned laser field to create potential hills between which the atoms are confined; some others [8,26] use optical lattices in order to create the atomic analog of DBR microcavities [27].

As it is well known from photon optics [6], if the frequency ω_L of the incident atom laser beam is far from resonance with all the cavity modes, the atomic beam is effectively forbidden from entering the cavity and therefore is nearly completely reflected back. On the other hand, if ω_L is close to the frequency ω_o of one of the cavity modes, this mode is resonantly excited: a substantial fraction of the incident atoms resonantly enter the cavity and are transmitted on the other side where they form the transmitted beam.

If we assume that the frequency spacing of the different cavity modes is much larger than both the laser linewidth and the atom-atom interaction energy, and if we suppose the atom laser frequency ω_L to be close to a cavity resonance, only this mode is effectively excited, while the other ones are safely neglected. If we develop the atomic field inside the cavity on its eigenstates

$$\hat{\psi}(x) = \sum_{\alpha} \phi_{\alpha}(x)\hat{c}_{\alpha}, \tag{1}$$

this *single-mode* approximation is equivalent to assuming all the $\hat{c}_{\alpha}$ to be effectively negligible but for one of them, which will be called in the following $\hat{a}$; let $\phi(x)$ be the wave function of such mode.

In this approximation, the Hamiltonian of the driven cavity can be written in the simple form [15,18]

$$\mathcal{H}=\hbar\omega_o\hat{a}^\dagger\hat{a}+\hbar\omega_{\rm nl}\hat{a}^\dagger\hat{a}^\dagger\hat{a}\hat{a}+i\hbar\beta_f\psi_i\hat{a}^\dagger e^{-i\omega_L t}+\text{H.c.}, \tag{2}$$

where $\hat{a}$ and $\hat{a}^\dagger$ are respectively the destruction and creation operators for the localized cavity mode. Thanks to the Bose nature of the atomic species under examination, such operators satisfy the usual Bose commutation relation $[\hat{a},\hat{a}^\dagger]=1$.

The first term of the Hamiltonian Eq. (2) describes linear oscillations at frequency ω_o; the second term keeps track of the (collisional) atom-atom interactions, whose strength is quantified by the $\omega_{\rm nl}$ parameter. This is easily related to the cavity mode wavefunction $\phi(x)$ and the *s*-wave scattering length a_o [28]:

$$\omega_{\rm nl}=\frac{2\pi\hbar a_o}{m}\int d^3x|\phi(x)|^4; \tag{3}$$

as expected, its sign is positive (negative) for repulsive (attractive) interactions. Since the atomic density inside the cavity is, at resonance, much larger than the density in the incident atom laser beam [6], atom-atom interactions outside the cavity are safely neglected; in addition, the single-mode approach neglects all those processes in which atoms are transferred from the mode $\hat{a}$ to the other modes of the cavity by the interactions; such an approximation is generally justified provided the interaction energy is much smaller than the spacing of adjacent cavity modes and parametric resonances of the kind $2\omega_\alpha=\omega_{\alpha'}+\omega_{\alpha''}$ are absent.

The driving of the cavity mode by the incident atom laser beam is taken into account by the last two terms. Thanks to the stationarity and all-order coherence assumptions discussed above, the driving field is well modeled as a monochromatic and classical ***C***-number field $\psi_i e^{-i\omega_L t}$ which forces the cavity mode to oscillate. In particular, the coupling coefficient β_f is proportional to the transmission amplitude of the front cavity mirror. Analogously, the amplitude of the transmitted field through the cavity $\hat{\psi}_{\rm tr}$ is proportional to the internal amplitude $\hat{a}$ times a κ_b coefficient proportional to transmission amplitude of the back mirror; all the statistical properties of the transmitted field can thus be expressed in terms of the internal field ones [15,22].

From the point of view of the sole cavity, the coupling to the continuum of propagating external modes through the nonperfectly reflecting mirrors, which underlies the driving of the cavity mode by the incident beam as well as the formation of the transmitted beam, is a dissipative process and thus cannot be included in a simple Hamiltonian formalism.

From the general theory of quantum damping [15,22], it follows that the dynamics of the single-mode cavity under examination is completely described by the following *master equation* for the density matrix $\hat{\rho}$,

$$\frac{\partial\hat{\rho}}{\partial t}=\frac{i}{\hbar}[\hat{\rho},\mathcal{H}]+\gamma D[\hat{a}]\hat{\rho}; \tag{4}$$

the first (Hamiltonian) term keeps track of the driving, the linear oscillations and the atom-atom interactions, while the second term keeps track of the dissipative effects. This latter has been written in terms of the superoperator $D[\hat{a}]\hat{\rho}$, defined as usual as

$$D[\hat{a}]\hat{\rho}=\hat{a}\hat{\rho}\hat{a}^\dagger-\tfrac{1}{2}(\hat{a}^\dagger\hat{a}\hat{\rho}+\hat{\rho}\hat{a}^\dagger\hat{a}); \tag{5}$$

the coefficient γ has the usual meaning of damping rate of the cavity excitation.

In the actual calculations, the steady-state of the density matrix $\hat{\rho}_{\rm eq}$ is determined by letting $\hat{\rho}$ evolve according to Eq. (4) for a time much longer than the characteristic relaxation time of the system under examination. The expectation values $\langle\hat{O}\rangle$ of the observables $\hat{O}$ of interest are calculated as mean values over the steady-state density matrix $\text{Tr}[\hat{\rho}_{\rm eq}\hat{O}]$; for the determination of a two-time correlation function $\langle\hat{O}_2(t)\hat{O}_1(0)\rangle$, we have to first apply the observable $\hat{O}_1$ to the left of $\hat{\rho}_{\rm eq}$, then let the resulting density matrix $\hat{O}_1\hat{\rho}_{\rm eq}$ evolve for a time t according to the master equation (4) and finally take the expectation value of second observable $\hat{O}_2$.

From a numerical point of view, several different representations can be chosen for $\hat{\rho}$ [15,17,29]; our actual simulations have been performed using a Fock representation in which the density matrix is expanded in the number-state basis $M_{n,n'}=\langle n|\hat{\rho}|n'\rangle$. The time evolution is numerically performed using a standard fourth-order Runge-Kutta method and then checking the numerical stability of the result with respect to a reduction in the integration time step.

In the case of symmetric systems, in which the front and back mirrors have the same transmission properties, the β_f,κ_b coefficients are related to the damping γ by the relations $\beta_f=(\gamma v/2)^{1/2}$ and $\kappa_b=(\gamma/2v)^{1/2}$, which follow from the well-known property that the transmission through any linear, symmetric and nonabsorbing cavity is, at exact resonance, exactly one (see, e.g., [30], Chap. 9); $v=(2\hbar\omega_o/m)^{1/2}$ denotes the (group) velocity of free atoms which coincide on the cavity at resonance.

Depending on the specific scheme adopted for the cavity, processes of different kinds can be responsible of additional incoherent nonradiative losses which are the atomic analog of light absorption in materials; in particular, if the confinement is a magnetic one, Majorana spin flips may occur, while spontaneous emission of light may take place in the presence of an optical confinement [31]. Such effects have to be handled by means of additional terms in Eq. (4) of the same form $\gamma_{\rm abs}D[\hat{a}]\hat{\rho}$: their main consequences are a broadening of the resonance and a reduction of the peak transmittivity by a factor $(\gamma+\gamma_{\rm abs})/\gamma$.

The single-mode nonlinear cavity model described in the present section has been widely applied to optical Fabry–Perot interferometers [14,18,32]: in that case, the field operator $\hat{a}$ describes an electromagnetic field instead of a matter field and the nonlinear interaction between photons results from the third-order nonlinear polarizability $\chi^{(3)}$ of the cavity material. The main difference consists in the strength of the nonlinear coupling, which can be quantified by the num-

ber $N_o=\gamma/\omega_{\rm nl}$ of quanta which are necessary for having an appreciable nonlinear effect on the transmittivity. Since the optical nonlinearity of usual materials is very weak, conventional optical resonators are characterized by $N_o \gg 1$, which means that a huge number of photons have to be excited inside the cavity before the effect of optical nonlinearity to be apparent; for this reason, such systems have been mostly studied within a mean-field approach with linearized fluctuations. Section III of the present article is devoted to a detailed discussion of the validity of such an approach: in particular, the approximated predictions of MFT are compared to the result of our exact numerical calculations and agreement is found in the classical $N_o \gg 1$ limit; in terms of the many-body theory of the interacting Bose gas, this condition would correspond to the classical diluteness condition $na_o^3 \ll 1$ (n being the spatial density of the 3D gas).

Only very recently, an active interest has been focused on the possibility of achieving the opposite $N_o \leqslant 1$ regime with light: optical materials with very strong nonlinearities as well as very high Q-valued cavities have been investigated in order to generate nonclassical states of the field and even entangled ones.

First of all, high finesse optical cavities containing a small number of atoms have been investigated in the realm of cavity quantum electrodynamics [11]: in this case, the nonlinearity mechanism is the intrinsic one of two-level atoms: with a smaller number of atoms, a smaller number of photons is required for the saturation of the transition, but at the same time the weaker polarizability imposes a stronger requirement on cavity finesse. Furthermore, an additional loss channel is introduced by the spontaneous decay of excited atoms.

Second, quantum coherence effects in multilevel atoms dressed by strong pump fields have been theoretically shown to give enhanced nonlinear susceptibilities as well as depressed absorptions [12,14]: despite the formal difficulties related to the complex internal dynamics of the three-level atoms [33,34], such arrangements are now beginning to be exploited for low intensity nonlinear optics experiments [13] as well as for the study of very slow pulse propagation [35].

Finally, new cavity geometries with enhanced Q-factors are also being investigated: in particular, the whispering gallery modes of cylindrical or spherical resonators look very promising, since fused silica spheres and disks with spatial sizes of the order of micrometer and very weak surface roughness are currently available; unfortunately, the nonlinear susceptibility of fused silica is very weak and the insertion of localized active impurities is generally necessary [10].

On the other hand, recent theoretical work on atomic Fabry-Perot interferometers [8] has shown that the use of spatially modulated optical lattices allows for well separated cavity modes with narrow linewidths and tight longitudinal confinement: in particular, it has been shown that atom-atom interactions can give rise to atom optical bistability with a very low threshold intensity of the order of 10^{13} at/cm^{2}s. Provided transverse motion is appropriately frozen by means of a single-mode atomic waveguide [25], such systems behave as effectively one-dimensional ones. Thanks to the transverse confinement, the isolated cavity resonance can show a nonlinear coupling $\omega_{\rm nl}$ comparable or even larger than the mode linewidth γ and therefore $N_o \leqslant 1$. In this regime, MFT breaks down and a full quantum calculation based on the master equation (4) is required; the peculiar coherence properties which result from the calculations will be discussed in Sec. IV.

With respect to optical systems, the Hamiltonian of the atomic FP cavity allows for a more transparent discussion of the quantum dynamics: the collisional nonlinearity for the atomic matter field is described by a simple quartic term in the field Hamiltonian, while in the case of strongly nonlinear optical media the internal dynamics of the atoms must generally be taken into account explicitly in the calculations.

III. WEAK NONLINEARITY CASE: MEAN-FIELD THEORY AND LINEARIZED FLUCTUATIONS

The approximation scheme most commonly used for the study of the dynamics of trapped atomic Bose-Einstein condensates (BEC) is certainly the mean-field theory [16]: the atomic field is described as a classical ***C***-number field equal to the mean value of the quantum field $\psi(\mathbf{x},t)=\langle\hat{\psi}(\mathbf{x},t)\rangle$ and factorization is assumed for the operator products involved in the motion equation of this macroscopic wavefunction; fluctuations are then treated in a linearized way by means of the Bogoliubov's technique.

Using the many-body theory of 3D Bose gases, this approach can be proven to give correct results in the case of dilute systems in which the density n is low enough for the mean interparticle distance $n^{-1/3}$ to be much larger than the scattering length a_o; current atomic samples well satisfy such a condition. In other terms, for a constant mean-field interaction energy (which is proportional to na_o), MFT is valid in the classical limit $a_o \to 0$ and $n \to \infty$, in which the discrete nature of the matter field is effectively washed out.

For the single-mode nonlinear interferometer described in the previous section, the mean-field approach leads to a single differential equation for the mean value of the cavity field $a(t)=\langle\hat{a}(t)\rangle$ of the form [15,18]

$$\frac{da}{dt}=-i(\omega_o+2\omega_{\rm nl}|a|^2)a+\beta_f\psi_i e^{-i\omega_L t}-\frac{\gamma}{2}a, \qquad (6)$$

from which we can immediately obtain the steady-state value $a(t)=\overline{a}e^{-i\omega_L t}$ with

$$\overline{a}=\frac{i\beta_f\psi_i}{\omega_L-\omega_o-2\omega_{\rm nl}|\overline{a}|^2+i\gamma/2}. \qquad (7)$$

If fluctuations of the cavity field are completely neglected, the transmitted field $\hat{\psi}_t=\kappa_b\hat{a}$ has the same all-order coherence properties as the incident one. Lowest-order fluctuations around the mean value can be taken into account just by solving the linearized [18] version of the stochastic equations of Positive-P representation [17]; this procedure is a sort of generalization of Bogoliubov's approach to driven dissipative systems.

Using the Positive-P representation of a quantum Bose field, it can be shown that the dynamics of the field in a nonlinear single-mode cavity is described by a pair of stochastic differential equations

$$d\alpha=\left[-i(\omega_o+2\omega_{\rm nl}\alpha^*\alpha)\alpha+\beta_f\psi_i e^{-i\omega_L t}-\frac{\gamma}{2}\alpha\right]dt + \sqrt{-2i\omega_{\rm nl}\alpha^2}\,d\eta_1, \tag{8}$$

$$d\alpha^*=\left[i(\omega_o+2\omega_{\rm nl}\alpha\alpha^*)\alpha^*+\beta_f^*\psi_i^* e^{i\omega_L t}-\frac{\gamma}{2}\alpha^*\right]dt + \sqrt{2i\omega_{\rm nl}\alpha^{*2}}\,d\eta_2 \tag{9}$$

for the field variables α and α^*, which are now complex conjugates of each other only in the mean. The noise terms $d\eta_i$ are independent Gaussian noise terms ($\overline{d\eta_i}=0$, $\overline{d\eta_i\,d\eta_j}=\delta_{i,j}dt$) [36]. In terms of the stochastic field variables α and α^*, the mean value of any normally ordered observable can be expressed as

$$\langle\hat{a}^{\dagger m}\hat{a}^m\rangle=\overline{\alpha^{*m}\alpha^m}. \tag{10}$$

Linearizing the stochastic Eqs. (8) and (9) around the steady-state $\alpha=\overline{a}e^{-i\omega_L t}$, $\alpha^*=\overline{a}^*e^{i\omega_L t}$ of the deterministic evolution, we get to a pair of linear stochastic equations for the slowly varying field fluctuations $\delta\alpha=\alpha e^{i\omega_L t}-\overline{a}$ and $\delta\alpha^*=\alpha^* e^{-i\omega_L t}-\overline{a}^*$

$$d\,\delta\alpha=\left[-i(-\Delta\omega+4\omega_{\rm nl}|\overline{a}|^2)\,\delta\alpha-2i\omega_{\rm nl}\overline{a}^2\,\delta\alpha^*-\frac{\gamma}{2}\delta\alpha\right]dt + \sqrt{-2i\omega_{\rm nl}\overline{a}^2}\,d\eta_1, \tag{11}$$

$$d\,\delta\alpha^*=\left[i(-\Delta\omega+4\omega_{\rm nl}|\overline{a}|^2)\,\delta\alpha^*+2i\omega_{\rm nl}\overline{a}^{*2}\,\delta\alpha-\frac{\gamma}{2}\delta\alpha^*\right]dt + \sqrt{2i\omega_{\rm nl}\overline{a}^{*2}}\,d\eta_2. \tag{12}$$

From these equations, all the stationary moments can be extracted using the standard techniques for the solution of linear stochastic differential equations [36]. We shall not reproduce here all the details of the calculations, which can be found in the original paper [18], but we shall only give the final results and compare them with the exact result of our numerical calculations.

As described in [18], the mean transmitted intensity is given by

$$I_{\rm tr}=v|\kappa_b|^2\langle\hat{a}^\dagger\hat{a}\rangle=\frac{\gamma}{2}\left[N+\frac{\omega_{\rm mf}^2}{2|\lambda(\omega_L)|}\right]=I_{\rm coh}+I_{\rm nc}; \tag{13}$$

the first term $I_{\rm coh}$, which describes the coherently (i.e., elastically) transmitted intensity, corresponds to the mean-field amplitude $\overline{a}$; the second one $I_{\rm nc}$ accounts for quantum fluctuations and thus describes the incoherently (inelastically) transmitted intensity. With $\Delta\omega=\omega_L-\omega_o$ we have denoted the detuning of the incident atom laser beam with respect to the empty cavity mode; $N=|\overline{a}|^2$ is the mean-field number of quanta in the cavity mode and $\omega_{\rm mf}=2\omega_{\rm nl}N$ is the corresponding frequency shift of the cavity mode; finally, for notational simplicity, we have set

$$\lambda(\omega)=\left\{i[(\omega-\omega_L)+(\Delta\omega-2\omega_{\rm mf})]+\frac{\gamma}{2}\right\}\cdot\left\{i[(\omega-\omega_L) -(\Delta\omega-2\omega_{\rm mf})]+\frac{\gamma}{2}\right\}-\omega_{\rm mf}^2. \tag{14}$$

As expected, for a fixed value of the mean-field interaction energy $\omega_{\rm mf}$, the contribution of fluctuations is inversely proportional to the number of atoms in the cavity mode and thus vanishingly small in the classical limit ($\omega_{\rm nl}\to 0$, $N\to\infty$). With a similar procedure we can determine the one-time second-order correlation function $g^{(2)}(0)$:

$$g^{(2)}(0)=\frac{\langle\hat{a}^\dagger\hat{a}^\dagger\hat{a}\hat{a}\rangle}{\langle\hat{a}^\dagger a\rangle}^2=1+\frac{\omega_{\rm mf}}{|\lambda(\omega_L)|N}(\Delta\omega-\omega_{\rm mf}). \tag{15}$$

Finally, a Fourier transform of the first-order correlation function leads to the spectrum of the transmitted intensity

$$S(\omega)=S_{\rm coh}(\omega)+S_{\rm nc}(\omega)=\frac{\gamma}{2}\mathcal{F}_t\langle\hat{a}^\dagger(t)\hat{a}(0)\rangle =\frac{\gamma}{2}\left\{N\delta(\omega-\omega_L)+\frac{\gamma\omega_{\rm mf}^2}{2\pi|\lambda(\omega)|^2}\right\} \tag{16}$$

in which we again recognize the elastic and inelastic contributions; the former corresponds to the delta-function peak at ω_L, while the latter gives a pair of (inelastic) Lorentzian peaks at the frequencies

$$\omega^\pm=\omega_L\pm\sqrt{\Delta\omega^2-4\Delta\omega\omega_{\rm mf}+3\omega_{\rm mf}^2}, \tag{17}$$

which correspond to the dressed states of the driven system. Poles at these same frequencies appear in the linear response of the driven system to additional probe beams [22,37,38]. Whenever the argument of the square root is negative, the two peaks coalesce into a single one at ω_L.

These results are to be compared to the exact solution of the full master equation (4) obtained using the numerical technique sketched in the previous section. In Fig. 2, we have plotted the coherent and the incoherent transmitted intensities $I_{\rm coh}$ and $I_{\rm nc}$ vs. the incident intensity $I_{\rm inc}=v|\psi_i|^2=(2/\gamma)|\beta_f\psi_i|^2$ for different values of the nonlinearity parameter $N_o=\gamma/\omega_{\rm nl}$ at zero detuning $\Delta\omega=0$. In the plots, the intensities (defined as the number of atoms per unit time flowing along the waveguide) have been normalized in units of the characteristic intensity $\gamma^2/\omega_{\rm nl}=\gamma N_o$, so that the mean-field curves for the coherently transmitted intensity superimpose on each other exactly.

In the zero detuning $\Delta\omega=0$ case we are considering, MFT [Eq. (7)] predicts an optical limiter [6] behavior for the transmitted intensity: for growing intensities, in fact, the mean-field interaction energy $2\hbar\omega_{\rm nl}|a|^2$ tends to shift the cavity mode out of resonance with respect to the incident beam and thus to lower the effective transmittivity. In par-

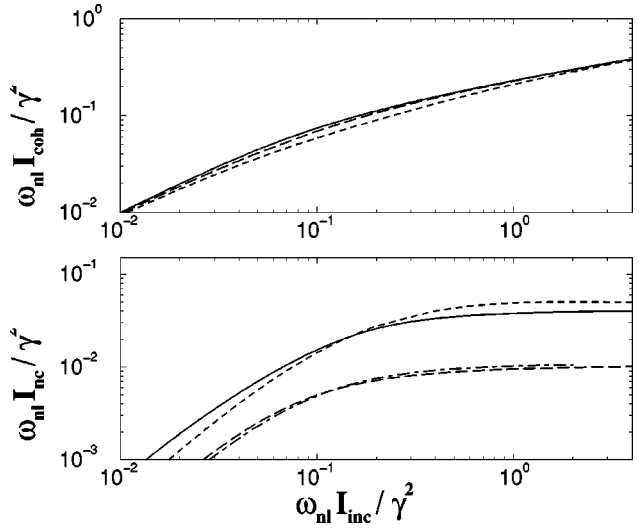

FIG. 2. Transmission properties of a nonlinear Fabry-Perot interferometer in the weak nonlinearity (large N_o) regime: in the upper panel, coherent intensity I_{coh} as a function of the incident intensity I_{inc}; in the lower one, incoherent intensity I_{nc}. All intensities have been normalized to the characteristic intensity $\gamma^2/\omega_{\mathrm{nl}}$. In the upper panel, the solid curve is the result of the linearized approach, while the long- and short-dashed ones correspond to the exact calculations for $N_o=8$ and $N_o=2$, respectively. In the lower panel, the solid and the long-dashed lines are again the approximate results, while the short-dashed and the dot-dashed are the exact ones. The upper curves are for $N_o=2$, the lower ones are for $N_o=8$.

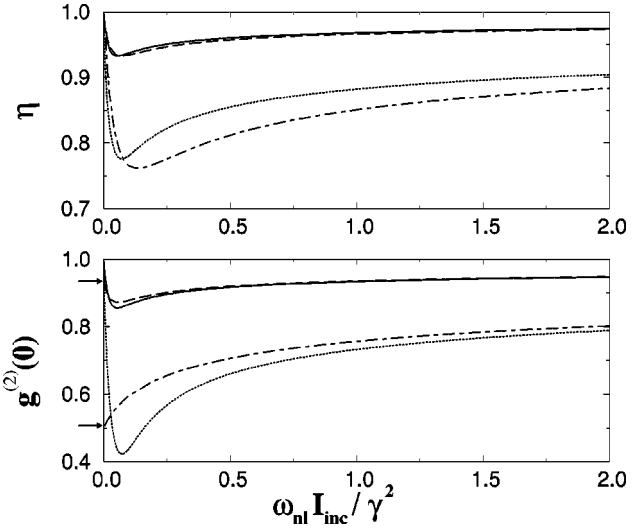

FIG. 3. Coherence properties of the transmitted beam as a function of the incident intensity I_{inc}: in the upper panel, long-time first-order coherence $\eta=I_{\mathrm{coh}}/I_{\mathrm{tr}}$; in the lower panel, one-time second-order coherence $g^{(2)}(0)=\langle \hat{a}^\dagger \hat{a}^\dagger \hat{a} \hat{a} \rangle / \langle \hat{a}^\dagger \hat{a} \rangle^2$. The solid and the dotted curves are the approximated results of linearized theory for $N_o=8$ and $N_o=2$, respectively, while the long-dashed and the dot-dashed are the exact ones for the same parameter choices. The arrows in the lower panel are the predictions of the analytical expression Eq. (21) for $g^{(2)}(0)$ in the low-intensity limit.

ticular, while at low intensity the transmitted intensity grows linearly with the incident intensity, in the large intensity limit the transmitted intensity grows only as its power 1/3. In a log-log scale, the transition between these two regimes can be observed as a rather smooth bending.

The discrepancy of the MF result for the coherently transmitted intensity with respect to the exact one is concentrated mostly in the crossover region and, as expected, tends to disappear in the classical limit $N_o \to \infty$ (see upper panel of Fig. 2). An analogous comparison can be made for the incoherently transmitted intensity (see lower panel of the same figure): at lowest order [Eq. (13)], such a quantity is a factor of N lower than the coherent contribution and thus its relative weight vanishes in the classical limit. As expected, the discrepancy of the MF result with respect to the exact one is of higher order in N_o^{-1}.

In the upper panel of Fig. 3, we have plotted the first-order long-time coherence of the transmitted beam

$$\eta = \frac{I_{\mathrm{coh}}}{I_{\mathrm{tr}}} = \frac{\lim_{t\to\infty} |\langle \hat{a}^\dagger(t) \hat{a}(0) \rangle|}{\langle \hat{a}^\dagger(0) \hat{a}(0) \rangle} \tag{18}$$

as a function of the (normalized) incident intensity for different values of N_o. All curves show a single minimum at a value of the incident intensity which, being related to the crossover in the optical limiter response curve, is approximately proportional to γN_o; the depth of such a minimum is approximately inversely proportional to N_o. Perfect coherence $\eta=1$ is recovered in the classical limit $N_o \to \infty$.

A similar behavior is found also for the one-time second-order coherence $g^{(2)}(0)$ which is plotted in the lower panel of the same figure; a value for $g^{(2)}(0)$ smaller than 1 means that the transmitted beam is antibunched, i.e., has reduced intensity fluctuations as compared to a classical coherent beam. Such a quantum property is a consequence of the optical limiter response and is at lowest order inversely proportional to N_o.

As previously, the MF result is found to keep track in a correct way of the lowest order fluctuations: the discrepancy with the exact result is in fact of higher order in N_o^{-1} for any incident intensity. In particular, for the low intensity limit $I_{\mathrm{inc}} \to 0$ the mean field theory predicts $g^{(2)} \to 1$ [see Eq. (15)], since in this regime the system behaves as an effectively linear one. On the other hand, the exact calculation gives a value lower than 1, which is an unambiguous signature of the discrete nature of the field: while the ***C***-number variable which describes the field in the linearized treatment can assume any value, the quantum system can only be in a discrete ladder of states. For an incident beam at exact resonance with the empty cavity, the $|n=1\rangle$ state is on resonance, while the second excited one $|n=2\rangle$ is already out of resonance of a finite frequency $2\omega_{\mathrm{nl}}$. A straightforward but somewhat lengthy analytical calculation for the steady-state value of the density matrix $\hat{\rho}_{\mathrm{eq}}$ at lowest order in I_{inc} leads to the expressions

$$\rho_{11}^{\mathrm{eq}} \simeq \frac{4|\beta_f \psi_i|^2}{\gamma^2} \tag{19}$$

and

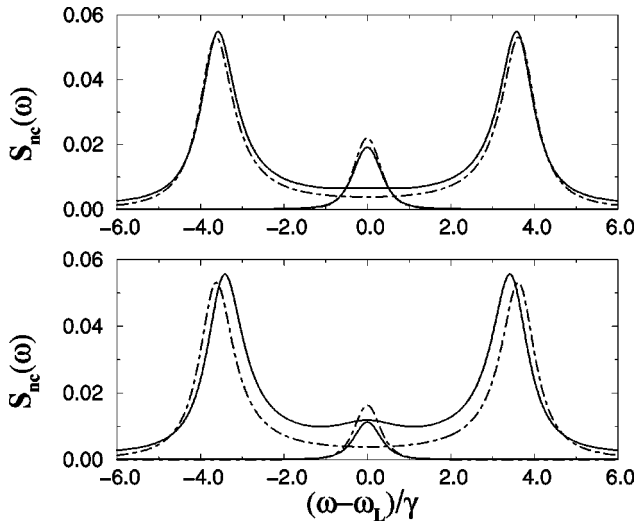

FIG. 4. Incoherently transmitted intensity spectra: in the upper panel, $N_o=8$; in the lower one, $N_o=2$. The solid lines refer to the exact calculations, while the dot-dashed ones are the result of the linearized approach. The incident intensities are equal to $I_{\rm inc}=0.24\gamma$ and $I_{\rm inc}=80\gamma$ for the upper panel spectra, and to $I_{\rm inc}=0.06\gamma$ and $I_{\rm inc}=20\gamma$ for the lower panel ones.

$$\rho_{22}^{\rm eq}\simeq\frac{8|\beta_f\psi_i|^4}{\gamma^2(\gamma^2+4\omega_{\rm nl}^2)} \tag{20}$$

for the matrix elements $\rho_{11}^{\rm eq}=\langle n=1|\hat{\rho}_{\rm eq}|n=1\rangle$ and $\rho_{22}^{\rm eq}=\langle n=2|\hat{\rho}_{\rm eq}|n=2\rangle$. From these expressions, it is immediate to obtain an expression of the one-time second-order coherence function

$$g^{(2)}(0)=\frac{2\rho_{22}^{\rm eq}}{(\rho_{11}^{\rm eq})^2}=\frac{1}{1+4/N_o^2}, \tag{21}$$

which is valid in the low-intensity limit for any value of N_o. This exact analytical prediction is marked with horizontal arrows in the lower panel of Fig. 3 and the agreement with the numerical result is excellent. As expected, in the classical $N_o\to\infty$ limit, the analytical expression Eq. (21) tends to the mean-field prediction of 1 and, at lowest order, the discrepancy is proportional to N_o^{-2}.

Finally, in Fig. 4 we have plotted a few spectra of the inelastically transmitted intensity in the zero detuning ($\Delta\omega=0$) case and we have compared the approximate result of MFT to the exact one. Apart from the small central peak at $\omega=\omega_L=\omega_o$ which appears at smaller values of N_o, both the position and the intensities of the external peaks as predicted by the MFT are in excellent agreement with the exact result. As previously, the larger the N_o parameter, the closer the similarity.

In the present article, we shall not specifically address the case of a detuned driving field $\Delta\omega\neq0$ and we shall limit ourselves to a few remarks. In the case where the detuning has opposite sign with respect to the nonlinear frequency shift of the cavity mode, the feedback of the nonlinearity on the transmission is still negative and leads to the same optical limiter behavior previously described; only the frequencies of the dressed modes in Eq. (17) are different. On the other hand, when the detuning has the same sign as the nonlinear shift, the feedback of the nonlinearity is positive and MFT predicts the possibility of multiple steady-state solutions of Eq. (7) for a single value of the incident intensity [6]. In this case, the linearized theory can account only for the fluctuations occurring in the neighborhood of each steady-state [18], but it does not keep track of effects related to quantum tunneling from one steady-state to another [15,39]. Nevertheless, the numerical solution of the full master equation (4), as it has been described in the present article, can provide us exact results for the coherence properties of the transmitted beam. Given their complexity, a complete discussion of these points is postponed to a forthcoming publication.

IV. STRONG NONLINEARITY: THE *ATOM BLOCKADE* EFFECT

In the previous section we have discussed the solution of the quantum master equation (4) in the weak nonlinearity $N_o\gg1$ regime in which the exact numerical solution is accurately approximated by the analytic mean-field result. In that case, in fact, the behavior of the quantum field has been shown to be well reproduced by a classical field while the discrete nature of the field was taken into account simply by means of noise terms in the stochastic motion equations (11) and (12). Unfortunately, an exact solution of the complete Positive-P equations (8) and (9) does not mathematically exist for small values of N_o because of the well-known divergences of the field amplitudes [40]. Since a relatively small value of N_o means that only a moderate number of Fock states are actually involved in the dynamics, a numerical calculation in the Fock basis can be easily performed within a short computation time; moreover, the results of the numerical calculations are themselves best understood in the number-state basis $|n\rangle$.

In this basis, the Hamiltonian of the driven nonlinear single-mode cavity has the form

$$\frac{\mathcal{H}}{\hbar}=\begin{pmatrix} 0 & \mathcal{E}_i e^{-i\omega_L t} & 0 & 0 & \\ \mathcal{E}_i^* e^{i\omega_L t} & \omega_o & \sqrt{2}\mathcal{E}_i e^{-i\omega_L t} & 0 & \\ 0 & \sqrt{2}\mathcal{E}_i^* e^{i\omega_L t} & 2\omega_o+2\omega_{\rm nl} & \sqrt{3}\mathcal{E}_i e^{-i\omega_L t} & \vdots \\ 0 & 0 & \sqrt{3}\mathcal{E}_i^* e^{i\omega_L t} & 3\omega_o+6\omega_{\rm nl} & \\ & & \cdots & & \end{pmatrix}, \tag{22}$$

where the Rabi frequency of the driving $|\mathcal{E}_i| = |\beta_f \psi_i|$ is determined by the incident intensity $I_{\rm inc} = (2/\gamma)|\mathcal{E}_i|^2$. For a vanishing driving incident intensity ($\mathcal{E}_i = 0$), the eigenvectors of $\mathcal{H}$ are the Fock states $|n\rangle$ themselves, and their eigenenergies are equal to $n\omega_o + n(n-1)\omega_{\rm nl}$; because of the presence of nonlinear interactions, the energy splitting of adjacent modes, given by $\omega_o + 2n\omega_{\rm nl}$, is a monotonically increasing (decreasing) function of n for repulsive (attractive) interactions.

In the zero-detuning ($\Delta\omega = 0$) case, only the transition $|n=0\rangle \rightarrow |n=1\rangle$ is on resonance with the driving field; indeed, the higher states are shifted off the n-atom resonance of a frequency $(n-1)\omega_{\rm nl}$. In particular, an incident intensity $I_{\rm inc}$ of the order of $8\omega_{\rm nl}^2/\gamma = 8\gamma/N_o^2$ is required for the Rabi frequency $|\mathcal{E}_i|$ to be equal to the detuning of the $|n=2\rangle$ level and thus for this to be effectively populated.

This physical picture is confirmed by the results of the numerical calculations reproduced in Figs. 5 and 6: for moderate intensities $I_{\rm inc} \ll I_2 = \gamma/N_o^2$, the cavity shows a behavior analogous to the one of a driven two-level system; in particular, the transmitted atomic beam has the same statistical properties as the resonance fluorescence from a single two-level atom [15,22].

Such an effect can be considered as a sort of atom optical analog of the well-known *Coulomb blockade* of microscopic electronic systems [19]: in this case, the electrostatic charging energy due the injection of a single carrier inside the device is able to bring the energy of the electronic states involved in transport above the Fermi level of the injector and therefore to forbid the injection of other carriers. In the atomic case, the collisional interaction energy following the presence of a single atom is able to shift the cavity mode frequency of an amount equal to $2\omega_{\rm nl}$. If the incident beam is initially on resonance with the cavity, and if we are in a strong nonlinearity regime $\omega_{\rm nl} \gg \gamma$, the entrance of a second atom in the cavity is an off-resonant process, and thus it is strongly suppressed. This means that before a second carrier can enter the cavity, the first one must have left. As usual, the antibunching of the transmitted beam which follows from this *atomic blockade* effect results in a suppression of intensity noise below the shot-noise limit.

There are, however, significant differences between the two cases: in the electronic case, the device is driven by a multimode and incoherent thermal gas, possibly Fermi-degenerate, and the transport of electrons involves a continuum of transverse electronic states so that the transmitted current is generally carried by transversally incoherent electrons. In order for the Coulomb blockade not to be destroyed by thermal effects, the energy position of the electronic states in the device after the injection of a single carrier has to differ from the Fermi energy of the injector by an amount much larger than the thermal energy. In the atomic case, a cavity with well-spaced discrete modes has been considered, which is driven by a coherent atom laser beam (of course, this is possible only with bosonic atoms); in this case, the transmitted beam maintains at least partially the coherence of the incident beam. In order for the atom blockade effect to be apparent, atom-atom interactions have to shift the cavity mode off-resonance from the incident atom laser by an amount much larger than both the atom laser and the cavity mode linewidths.

For strong nonlinearities ($N_o \ll 1$), the characteristic incident intensity scale $I_{\rm sat}$ for the saturation of the two-level system, which is of the order of γ, is well separated from the characteristic intensity $I_2 = \gamma/N_o^2$ for substantial population of the $|n=2\rangle$ state. Hence it exists an intensity window $I_{\rm sat} \ll I_{\rm inc} \ll I_2$ in which the two-level system is effectively saturated but the higher excited states are still unpopulated: in this window the atom blockade is most effective in imposing the strict upper limit $I_{\rm tr} \leqslant \gamma/4$ to the total transmitted intensity. In this same intensity window, the spectral distribution of the transmitted intensity is characterized by the usual coherent delta-like peak at ω_L due to coherent (elastic) transmission plus a triplet of peaks (the so-called Mollow triplet [41]) resulting from incoherent transmission (see Fig. 6).

Physical behaviors of this kind are, however, very general, since they follow from the structure of the spectrum of the system: if the spacing of the levels is far from being uniform, a driving which is resonant with the lowest lying transition cannot excite the higher ones except at large values of its intensity, so that the system effectively behaves as a two-level one. This behavior is found, e.g., in the optical response of atoms, for which a two-level approximation is generally justified by the fact that the higher-lying optical transitions have frequencies much different from the fundamental one. Also cavity QED systems containing a few atoms [11] as well as cavity electromagnetically induced transparency [34] can give rise to effective two-level systems under appropriate conditions for which the spacing of the lowest-lying dressed states is significantly different from the spacing of the higher ones.

The intensity scale separation $I_{\rm sat} \ll I_2$ translates into the characteristic dependence of the total transmitted intensity on the incident intensity that can be observed in the upper panel of Fig. 5. First of all, when the two-level system is not saturated, the transmitted intensity is a linear function of the incident one; then, for $I_{\rm inc}$ of the order of γ, saturation of the two-level system occurs and the response flattens. Finally, for $I_{\rm inc}$ of the order of γ/N_o^2, the transmitted intensity starts to grow again thanks to the contribution of the $|n=2\rangle$ state.

The behavior of the single coherent and incoherent contributions to the transmitted intensity as functions of the incident intensity can also be interpreted within this same picture. As in the classical two-level system [22], at low incident intensities most of the transmission is coherent, since the coherent fraction $I_{\rm coh}$ is a linear function of $I_{\rm inc}$ and the incoherent fraction $I_{\rm nc}$ a quadratic one. When the two-level system is appreciably saturated, the incoherent fraction starts to dominate, while the coherent one drops to nearly zero. As the incident intensity grows even further, more than one atom can be simultaneously stored in the cavity mode, so that the $|n=2\rangle$ state is populated as well; therefore the coherent component starts to grow again, while the incoherent one starts to decrease. In other terms, the first-order coherence η shows a minimum as a function of the incident intensity at a value corresponding to the saturation plateau of the two-level transition. The population of the $|n=2\rangle$ state can be singled out just by looking at the one-time second-

order coherence function $g^{(2)}(0)$. For the ideal two-level system, this quantity is rigorously zero for any value of $I_{\rm inc}$; any departure from this value is an unambiguous signature of a population of the $|n\geqslant 2\rangle$ levels. For low incident intensities $g^{(2)}(0)$ has the very small value $N_o^2/4$ [see Eq. (21)], while it is substantially larger than zero only above the saturation plateau.

In order to explain the incoherent transmission spectra reproduced in Fig. 6, it can be useful to apply the dressed states technique to the physical system formed by the cavity plus the driving field [22,23]. In analogy to what is usually done in the dressed atom model, we shall label the quantum states of such a system with a pair of integer numbers $(\mathcal{N},n)$, respectively denoting the number of atoms in the driving field and in the cavity mode. In the dressed atom model, the integer number n is generally replaced by a discrete index running over the different internal states of the fluorescing atom and $\mathcal{N}$ has the physical meaning of number of photons in the incident laser beam.

Neglecting for the moment the radiative damping of the cavity mode, the total number of atoms $N_T=\mathcal{N}+n$ is a conserved quantity; since $\mathcal{N}$ is assumed to be very large, adjacent manifolds have the same structure and are spaced from each other by an amount equal to the incident laser frequency ω_L; in particular, the corresponding eigenstates only differ for the number $\mathcal{N}$ of atoms in the driving field. Within each constant N_T manifold, the Hamiltonian of the dressed system in the Fock $|n\rangle$ basis has the simple form

$$\frac{\mathcal{H}}{\hbar}=\begin{pmatrix} 0 & \mathcal{E}_i & 0 & 0 & \\ \mathcal{E}_i^* & -\Delta\omega & \sqrt{2}\mathcal{E}_i & 0 & \\ 0 & \sqrt{2}\mathcal{E}_i^* & -2\Delta\omega+2\omega_{\rm nl} & \sqrt{3}\mathcal{E}_i & \vdots \\ 0 & 0 & \sqrt{3}\mathcal{E}_i^* & -3\Delta\omega+6\omega_{\rm nl} & \\ & & \cdots & & \end{pmatrix}. \tag{23}$$

As it is sketched in Fig. 7(a), transitions between one manifold to the immediately lower one occur because of radiative losses through the nonperfectly reflecting mirrors and give rise to the incoherent component of the transmitted beam. Denoting with ω_α the energy of the $|\psi_\alpha\rangle$ eigenstate of a manifold, we expect that the spectrum of incoherently transmitted atoms will be peaked at the frequencies $\omega_L+(\omega_\alpha-\omega_\beta)$; the intensity of each peak is proportional to the matrix element of the corresponding transition $|\langle\psi_\alpha|\hat{a}|\psi_\beta\rangle|^2$ times the population N_α of the departure level $|\psi_\alpha\rangle$.

For moderate intensities $I_{\rm inc}\ll\gamma/N_o^2$ the mixing of the bare states into the new dressed states is limited to the two lowest states of the manifold, while the upper states nearly coincide with the $|n\geqslant 2\rangle$ states and are nearly unpopulated; for this reason transitions involving these upper states give a negligible contribution to the incoherent transmission spectra. In this regime, these spectra are thus the usual Mollow spectra of resonance fluorescence from driven two-level systems: at very low intensity, there is a single peak at ω_o; for intensities at least of the order of the saturation intensity $|\mathcal{E}_i|\simeq\gamma$, there starts to be a symmetric triplet of peaks at respectively

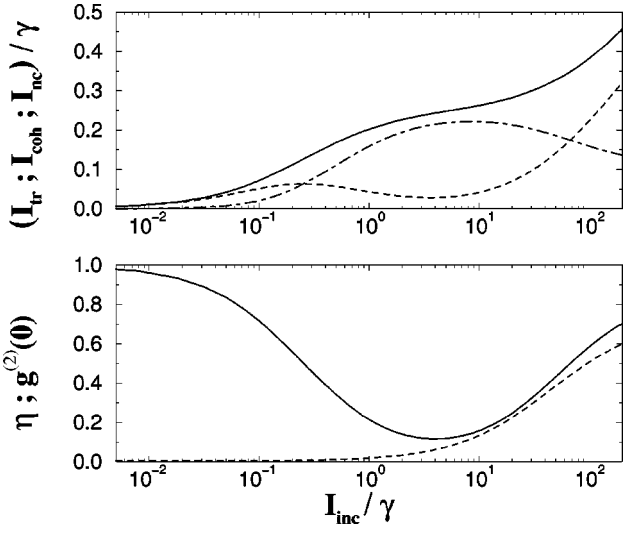

FIG. 5. Transmission and coherence properties of a nonlinear Fabry–Perot interferometer in the strong nonlinearity regime ($N_o=0.125$) as a function of the incident intensity: in the upper panel, transmitted intensity $I_{\rm tr}$ (solid line), coherent $I_{\rm coh}$ (dashed line) and incoherent $I_{\rm nc}$ (dot-dashed) components. In the lower panel, long-time first-order coherence η (solid line) and one-time second-order coherence $g^{(2)}(0)$ (dashed line). *Atom blockade* behavior occurs for $I_{\rm inc}$ comprised between $I_{\rm sat}=\gamma$ and $I_2=64\gamma$.

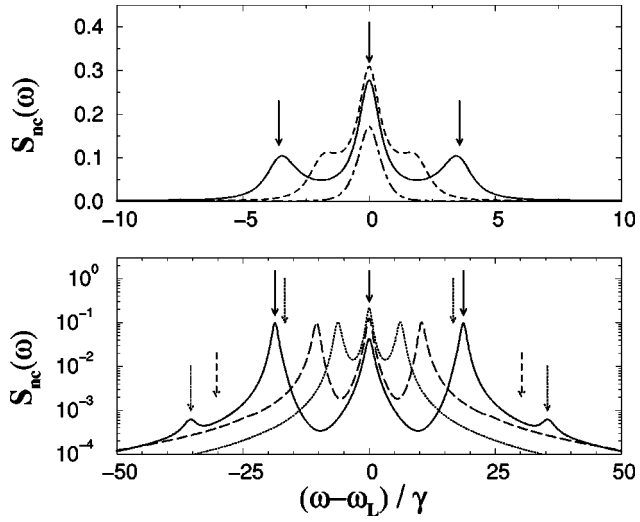

FIG. 6. Incoherently transmitted intensity spectra in the strong nonlinearity regime ($N_o=0.125$) for growing values of the incident intensity: in the upper panel, $I_{\rm inc}/\gamma=0.2,2,6.5$; in the lower one, $I_{\rm inc}/\gamma=20,60,240$. The arrows correspond to the transition frequencies resulting from the dressed cavity approach; the chosen parameters are the same ($I_{\rm inc}/\gamma=6.5,240$) as for the solid line spectra. In the lower panel, solid arrows correspond to transitions involving only the $|n=0,1\rangle$ states, while the dotted and dashed ones correspond to weaker transitions which involve respectively the $|n=2\rangle$ and the $|n=3\rangle$ states.

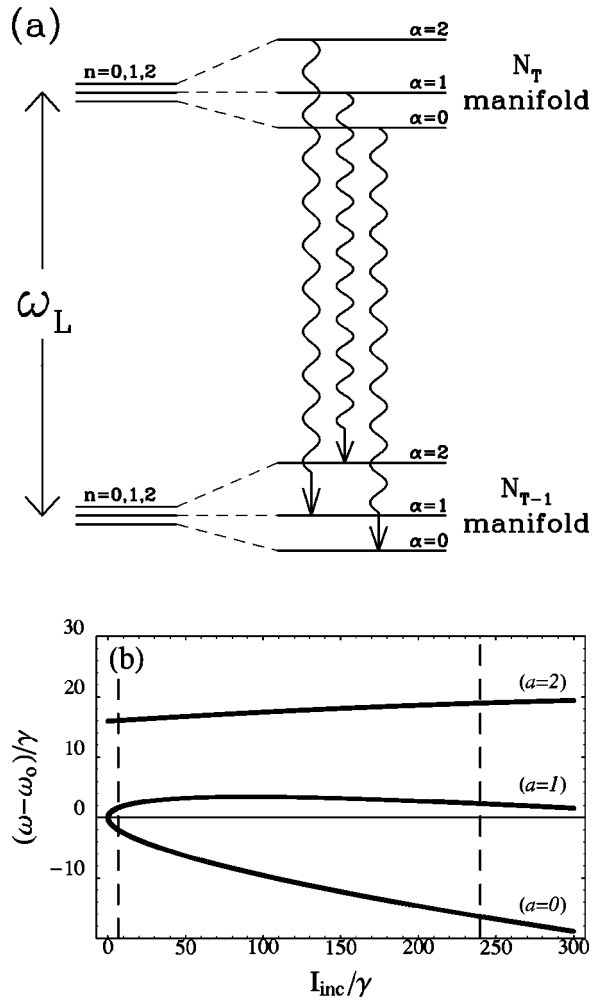

FIG. 7. Strong nonlinearity regime ($N_o=0.125$): sketch of the dressed cavity level scheme (panel a); dressed state frequencies (panel b) as a function of the incident intensity $I_{\rm inc}$ for the $\Delta\omega=0$ case. The vertical dashed lines correspond to the intensity values used in Fig. 6.

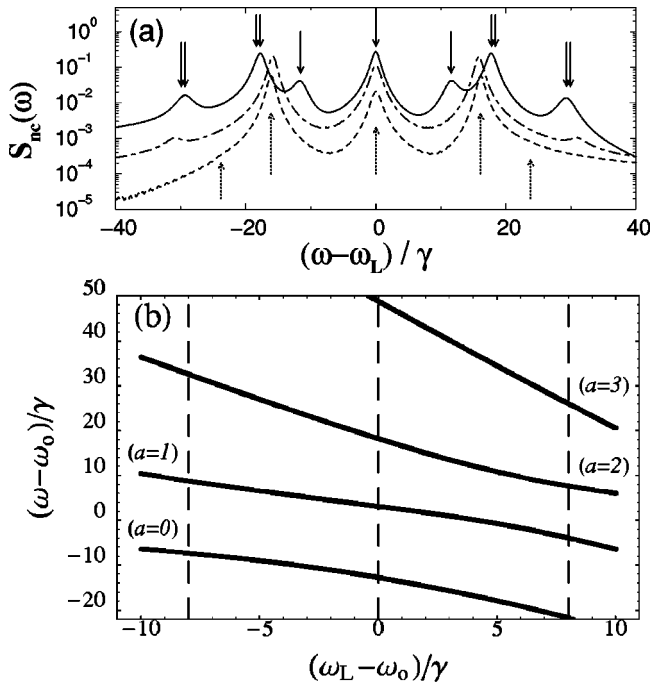

FIG. 8. Effect of a finite detuning $\Delta\omega$ on the incoherently transmitted intensity spectra in the strong nonlinearity regime ($N_o=0.125$, $I_{\rm inc}=160\gamma$): in the upper panel, spectra for $\Delta\omega/\gamma=-8,0,8$ (respectively, dashed, dot-dashed and solid lines); arrows indicate the transition frequencies according to the dressed cavity model: solid arrows refer to the $\Delta\omega/\gamma=8$ spectrum, dotted arrows to the $\Delta\omega/\gamma=-8$ one. In the lower panel, plot of the dressed state frequencies as function of the detuning $\Delta\omega$. The vertical dashed lines correspond to the values of the detuning which have been used in panel (a).

ω_o and $\omega_o\pm|\mathcal{E}_i|$, the central peak having a height three time larger than the lateral ones [see Fig. 6(b)].

At stronger intensities, when a larger number of states of the cavity begins to be effectively populated, the structure of the manifolds becomes more complex and additional peaks can be found in the wings of the fluorescence spectra; the stronger the driving field, the larger the mixing of $|n\geqslant 2\rangle$ states with the lower ones and, consequently, the stronger the intensity of the peaks corresponding to transitions involving such states.

A simple numerical diagonalization of the Hamiltonian Eq. (23) gives the frequencies of the peaks: in Fig. 7(b) we have reproduced the dependence of the frequency of the lowest dressed states on the driving strength. Obviously, since the higher state population is very small as well as the matrix elements of the transitions reaching them, only a few peaks are visible in the actual spectra plotted in Fig. 6. Comparison between the two approaches is easily made: the transition frequencies as they are predicted by the dressed state picture have been marked by vertical arrows; the agreement with the numerical peaks is excellent. Solid arrows refer to the transitions involving only $|n=0\rangle$ and $|n=1\rangle$, which are visible at any intensity. On the other hand, dotted (dashed) arrows denote transitions which involve the $|n=2\rangle$ ($|n=3\rangle$) state as well; given their weakness, the corresponding peaks can be distinguished from the underlying pedestal only at high intensities.

Remarkably, the intensity of the central peak at ω_o decreases for growing intensity with respect to the first pair of side peaks: this evolution suggests a smooth transition towards the two-peaked spectra obtained by means of the semiclassical approach described in the previous section; at very high driving intensity, in fact, when the mean occupation number of the cavity is much larger than one, fluctuations result again well described by the linearized theory of the previous section.

The dressed cavity model can be extended to the case of a nonvanishing detuning $\Delta\omega$ as well: the positions of the peaks are again well reproduced in terms of transitions connecting dressed states of adjacent manifolds. In the upper panel of Fig. 8 we have plotted a series of spectra for different detunings: the spectra are centered at the incident frequency ω_L, i.e., the spacing between adjacent manifolds.

When $\Delta\omega$ and $\omega_{\rm nl}$ have opposite signs, the nonlinear feedback on transmission is negative and the population of the upper states of the manifold is further reduced with re-

spect to the $\Delta\omega=0$ case; the lateral peaks in the spectra are therefore even weaker. On the other hand, when $\Delta\omega$ and $\omega_{\rm nl}$ have the same sign and the nonlinear feedback is positive, the population of the upper states of the manifold is enhanced and the spectra show a larger number of peaks. As previously, their frequencies result in good agreement with the predictions of the dressed cavity model, which are marked with arrows in the figure. In the lower panel of the same Fig. 8, we have specifically plotted the position of the different dressed states as functions of the detuning as they have been determined by numerically diagonalizing the Hamiltonian Eq. (23).

V. CONCLUSIONS AND PERSPECTIVES

In the present article we have investigated the nonlinear atom optical effects which arise from atom-atom collisional interactions in a single-mode atomic Fabry-Perot cavity driven by a coherent atom laser beam; in particular, we have numerically solved the full quantum master equation in a number-state basis and we have given a physical interpretation of the obtained results.

Provided the nonlinear interaction energy per atom is small, the exact results are well reproduced by the mean-field theory in which the atomic field is described as a classical ***C***-number field and quantum fluctuations are taken into account using a linearized version of the stochastic differential equations of Positive-P representation.

In the opposite limit of strong nonlinearity, the mean-field theory breaks down; for an incident beam exactly on resonance with the empty cavity, a sort of *atom blockade* effect is predicted: the presence of a single atom in the cavity mode pushes the mode frequency off-resonance from the incident field so that a second atom cannot enter the cavity but at very large incident intensities. The statistical properties predicted by the numerical calculations are very similar to the resonance fluorescence ones from a two-level system. A very strong incident beam is necessary for several atoms to be simultaneously forced into the cavity mode; this is reflected in a peculiar behavior of the transmitted intensity, a function of the incident intensity. The multiplet of peaks which characterizes the spectral distribution of the incoherently transmitted atoms can be interpreted as arising from radiative transitions between dressed states of the driven cavity: the agreement between the predictions of the dressed cavity model and the frequencies of the numerical peaks is excellent.

Although all the discussion has been focused on the case of an atomic Fabry-Perot cavity, similar results hold for an optical resonator filled with a nonlinear medium; in this case, since the intrinsic optical nonlinearity of current materials is generally very weak, clever schemes have to be adopted in order to enhance the nonlinear coupling per photon and depress losses so to attain the quantum $N_o \leqslant 1$ regime. On the other hand, the Fabry-Perot cavity for atomic matter waves proposed in [8] is expected to be already close to this condition.

As a following step, we plan to address the problem of atom optical bistability in the strong nonlinearity regime; in this case, the stationary state of the system corresponds to a density matrix which is a statistical mixture of the ''transmitting'' and ''nontransmitting'' steady-states of mean-field theory. Since quantum tunneling from one steady-state to the other may be effective on a time scale comparable to the cavity damping time γ, the transmitted beam is expected to show peculiar statistical properties.

ACKNOWLEDGMENTS

It is my greatest pleasure to thank G. C. La Rocca, whose suggestions have been illuminating during all the development of the present work. I am grateful to J. Dalibard and Y. Castin for continuous encouragement and hospitality at the Laboratoire Kastler-Brossel in Paris. I wish to thank A. Minguzzi and G. Ferrari for stimulating discussions.

[1] M. H. Anderson *et al.*, Science **269**, 198 (1995); K. B. Davis *et al.*, Phys. Rev. Lett. **75**, 3969 (1995); C. C. Bradley, C. A. Sackett, J. J. Tollett, and R. G. Hulet, *ibid.* **75**, 1687 (1995).

[2] H. M. Wiseman, Phys. Rev. A **56**, 2068 (1997); M. O. Mewes *et al.*, Phys. Rev. Lett. **78**, 582 (1997); I. Bloch *et al.*, *ibid.* **82**, 3008 (1999); E. W. Hagley *et al.*, Science **283**, 1706 (1999).

[3] L. Deng, E. W. Hagley, J. Wen, M. Trippenbach, Y. Band, P. S. Julienne, J. E. Simsarian, K. Helmerson, S. L. Rolston, and W. D. Phillips, Nature (London) **398**, 218 (1999).

[4] G. Lenz, P. Meystre, and E. M. Wright, Phys. Rev. Lett. **71**, 3271 (1993); Phys. Rev. A **50**, 1681 (1994); O. Zobay, S. Pötting, P. Meystre, and E. M. Wright, *ibid.* **59**, 643 (1999); K. J. Schernthanner, G. Lenz, and P. Meystre, *ibid.* **50**, 4170 (1994).

[5] W. Zhang and D. F. Walls, Phys. Rev. A **49**, 3799 (1994); **52**, 4696 (1995).

[6] R. W. Boyd, *Nonlinear Optics* (Academic Press, London, 1992).

[7] M. Trippenbach, Y. B. Band, and P. Julienne, Opt. Express **3**, 530 (1998); E. V. Goldstein and P. Meystre, Phys. Rev. A **59**, 1509 (1999).

[8] I. Carusotto and G. C. La Rocca, Phys. Rev. Lett. **84**, 399 (2000); *Bose-Einstein Condensates and Atom Lasers*, edited by S. Martellucci, A. N. Chester, A. Aspect, and M. Ingucio (Kluwer Academic/Plenum, New York, 2000), p. 153.

[9] M. Wilkens *et al.*, Phys. Rev. A **47**, 2366 (1993).

[10] V. B. Braginsky, M. L. Gorodetsky, and V. S. Ilchenko, Phys. Lett. A **137**, 393 (1989); L. Collot, V. Lefèvre-Seguin, M. Brune, J. M. Raimond, and S. Haroche, Europhys. Lett. **23**, 327 (1993).

[11] See the articles in *Cavity Quantum Electrodynamics*, edited by P. R. Berman (Academic Press, New York, 1993).

[12] H. Schmidt and A. Imamoglu, Opt. Lett. **21**, 1936 (1996); G. S. Agarwal and W. Harshawardhan, Phys. Rev. Lett. **77**, 1039 (1996); W. Harshawardhan and G. S. Agarwal, Phys. Rev. A **53**, 1812 (1996).

[13] S. E. Harris and Y. Yamamoto, Phys. Rev. Lett. **81**, 3611 (1999); S. E. Harris and L. V. Hau, *ibid.* **82**, 4611 (1999).
[14] A. Imamoglu, H. Schmidt, G. Woods, and M. Deutsch, Phys. Rev. Lett. **79**, 1467 (1997); Y. Yamamoto, Nature (London) **390**, 17 (1997).
[15] D. F. Walls and G. J. Milburn, *Quantum Optics* (Springer-Verlag, Berlin, 1994).
[16] F. Dalfovo, S. Giorgini, L. P. Pitaevskii, and S. Stringari, Rev. Mod. Phys. **71**, 463 (1999).
[17] P. D. Drummond and C. W. Gardiner, J. Phys. A **13**, 2353 (1980).
[18] P. D. Drummond and D. F. Walls, J. Phys. A **13**, 725 (1980).
[19] L. J. Geerligs *et al.*, Phys. Rev. Lett. **64**, 2691 (1990); A. Imamoglu and Y. Yamamoto, *ibid.* **70**, 3327 (1993); M. Reznikov *et al.*, *ibid.* **75**, 3340 (1995); J. Kim, H. Kan, and Y. Yamamoto, Phys. Rev. B **52**, 2008 (1995); J. Kim, O. Benson, H. Kan, and Y. Yamamoto, Nature (London) **397**, 500 (1999).
[20] M. Dagenais and L. Mandel, Phys. Rev. A **18**, 2217 (1978).
[21] R. Loudon, *The Quantum Theory of Light* (Clarendon, Oxford, 1983).
[22] C. Cohen-Tannoudji, J. Dupont-Roc, and G. Grynberg, *Processus d'Interaction entre Photons et Atomes* (InterEditions/ Editions du CNRS, Paris, 1988).
[23] C. Cohen-Tannoudji and S. Reynaud, J. Phys. B **10**, 345 (1977).
[24] J. Stenger *et al.*, Phys. Rev. Lett. **82**, 4569 (1999); E. W. Hagley *et al.*, *ibid.* **83**, 3112 (1999); I. Bloch, T. W. Hänsch, and T. Esslinger, Nature (London) **403**, 166 (2000).
[25] M. J. Renn *et al.*, Phys. Rev. Lett. **75**, 3253 (1995); D. Müller *et al.*, Phys. Rev. A **61**, 033 411 (2000); J. Fortagh *et al.*, Phys. Rev. Lett. **81**, 5310 (1998); J. Denschlag *et al.*, *ibid.* **82**, 2014 (1999); D. Müller *et al.*, *ibid.* **83**, 5194 (1999).
[26] L. Santos and L. Roso, Phys. Rev. A **58**, 2407 (1998); **60**, 2312 (1999).
[27] See the articles in *Confined Electrons and Photons*, edited by C. Weisbuch and E. Burstein (Plenum Press, New York, 1995).
[28] G. J. Milburn, J. Corney, E. M. Wright, and D. F. Walls, Phys. Rev. A **55**, 4318 (1997).
[29] K. Vogel and H. Risken, Phys. Rev. A **39**, 4675 (1989).
[30] W. H. Steel, *Interferometry* (Cambridge University Press, Cambridge, 1967).
[31] C. S. Adams and E. Riis, Prog. Quantum Electron. **21**, 1 (1997).
[32] D. F. Walls, P. D. Drummond, and K. J. McNeil, in *Optical Bistability*, edited by C. M. Bowden, M. Ciftan, and H. R. Robl (Plenum Press, New York, 1981), p. 51.
[33] M. D. Lukin, M. Fleischhauer, M. O. Scully, and V. L. Velichansky, Opt. Lett. **23**, 295 (1998); P. Grangier, D. F. Walls, and K. M. Gheri, Phys. Rev. Lett. **81**, 2833 (1998); A. Imamoglu, H. Schmidt, G. Woods, and M. Deutsch, *ibid.* **81**, 2836 (1998); K. M. Gheri, W. Alge, and P. Grangier, Phys. Rev. A **60**, R2673 (1999).
[34] M. J. Werner and A. Imamoglu, Phys. Rev. A **61**, 011801(R) (2000).
[35] L. V. Hau *et al.*, Nature (London) **397**, 597 (1999).
[36] C. W. Gardiner, *Handbook of Stochastic Methods* (Springer-Verlag, Berlin, 1983).
[37] I. Carusotto and G. C. La Rocca, Phys. Rev. B **60**, 4907 (1999).
[38] P. Alsing, D.-S. Guo, and H. J. Carmichael, Phys. Rev. A **45**, 5135 (1992).
[39] K. Vogel and H. Risken, Phys. Rev. A **38**, 2409 (1988).
[40] A. Gilchrist, C. W. Gardiner, and P. D. Drummond, Phys. Rev. A **55**, 3014 (1997).
[41] B. R. Mollow, Phys. Rev. **188**, 1969 (1969).